



Ceriotti, M. and McInnes, C.R. (2010) A near term pole-sitter using hybrid solar sail propulsion. In: 2nd International Symposium on Solar Sailing, ISSS 2010, 20-22 July 2010, New York, USA.

<http://strathprints.strath.ac.uk/20207/>

Strathprints is designed to allow users to access the research output of the University of Strathclyde. Copyright © and Moral Rights for the papers on this site are retained by the individual authors and/or other copyright owners. You may not engage in further distribution of the material for any profitmaking activities or any commercial gain. You may freely distribute both the url (<http://strathprints.strath.ac.uk>) and the content of this paper for research or study, educational, or not-for-profit purposes without prior permission or charge. You may freely distribute the url (<http://strathprints.strath.ac.uk>) of the Strathprints website.

Any correspondence concerning this service should be sent to The Strathprints Administrator: [eprints@cis.strath.ac.uk](mailto:eprints@cis.strath.ac.uk)

# A NEAR TERM POLE-SITTER USING HYBRID SOLAR SAIL PROPULSION

Matteo Ceriotti, Colin McInnes

Advanced Space Concepts Laboratory, Department of Mechanical Engineering  
University of Strathclyde, Glasgow G1 1XJ, United Kingdom

[matteo.ceriotti@strath.ac.uk](mailto:matteo.ceriotti@strath.ac.uk)

## ABSTRACT

In this paper we investigate optimal pole-sitter orbits using hybrid solar sail and solar electric propulsion (SEP). A pole-sitter is a spacecraft that is constantly above one of the Earth's poles. Optimal orbits, that minimize propellant mass consumption, are designed using a shape-based first guess followed by an optimal control problem solved with a direct method. SEP and hybrid spacecraft are compared in terms of payload mass fraction and mission lifetime, investigating the conditions under which the hybrid sail allows saving on the spacecraft initial mass. It is proposed that a hybrid solar sail and SEP system may be a means of enabling challenging long-duration, high energy missions by using a modest solar sail to enhance the performance of existing SEP technology.

## INTRODUCTION

The idea of hybridize solar sail propulsion and solar electric propulsion (SEP) on the same spacecraft is relatively new [1] and almost completely unexplored. The two propulsion systems complement each other, in terms of reliability and capabilities, enabling a whole new range of missions in which a continuous low thrust is required. Current research in this field ranges from artificial equilibria in the Sun-Earth system for Earth observation [2] to interplanetary transfers [3], to displaced periodic orbits in the Earth-Moon system [4]. Recently a hybrid sail demonstrator has been developed [5].

In this paper, we design optimal orbits for a hybrid pole-sitter mission. A pole-sitter is a spacecraft that is constantly above one of the Earth's poles [6]. It can provide a platform for continuous, real-time, medium-resolution observation of the Earth poles, with a full hemispheric view, and could enable a wide range of new applications, including monitoring of the ice cover and line-of-sight telecommunications to high-latitude regions. We will present the dynamical model, followed by a summary of the optimization procedure, and finally a mass budget in which the hybrid spacecraft and the pure SEP spacecraft will be compared in terms of payload mass fraction delivered and mission lifetime.

## 1. EQUATIONS OF MOTION

The circular restricted three-body problem (CR3BP) framework is considered (Sun-Earth-spacecraft). As is common, a synodic reference frame is used (Fig. 1a). The mass of the Sun and the Earth are denoted  $m_1$  and  $m_2$  respectively, and  $\boldsymbol{\omega} = \omega \hat{\mathbf{z}}$  the angular velocity of the system. The equations that describe the motion of the spacecraft of mass  $m$  in this system are:

$$\ddot{\mathbf{r}} + 2\boldsymbol{\omega} \times \dot{\mathbf{r}} + \boldsymbol{\omega} \times (\boldsymbol{\omega} \times \mathbf{r}) = -\nabla \left( \frac{1-\mu}{r_1} + \frac{\mu}{r_2} \right) + \mathbf{a}_s + \mathbf{T}/m \quad (1)$$

where  $\mathbf{r}$  is the position vector,  $\mathbf{a}_s$  is the acceleration due to the solar radiation pressure on the spacecraft sail,  $\mathbf{T}$  is the thrust provided by the solar electric propulsion (SEP) system.

Equation (1) will be used in its canonical non-dimensional form, that is assuming  $\omega = 1$ ,  $\mu = m_2 / (m_1 + m_2)$ , and the unit of distance being the separation of the two primaries. With these assumption, the position along the  $\hat{x}$ -axis of  $m_1$  is  $-\mu$ , and the position of  $m_2$  is  $1 - \mu$ . For the Earth-Sun system,  $\mu = 3.0404 \cdot 10^{-6}$ . The two vectors  $\mathbf{r}_1$  and  $\mathbf{r}_2$  represent the position of the spacecraft with respect to the Sun and the Earth respectively (see Fig. 1a).

The acceleration provided by a partially perfectly reflective, partially absorbing solar sail of total area  $A$  can be expressed as [7]:

$$\mathbf{a}_s = \frac{1}{2} \beta_0 \frac{m_0}{m} \frac{1-\mu}{r_1^2} \left[ g \cos \alpha \hat{\mathbf{n}} + h \sin \alpha \hat{\mathbf{t}} \right] \cos \alpha = \frac{1}{2} \beta_0 \frac{m_0}{m} \frac{1-\mu}{r_1^2} \sqrt{g^2 \cos^2 \alpha + h^2 \sin^2 \alpha} \cos \alpha \hat{\mathbf{m}}$$

Here  $\hat{\mathbf{n}}$  is the component normal to the sail and parallel  $\hat{\mathbf{t}}$  to it, in the plane of the Sun vector.  $\beta_0$  is the *lightness number* at the beginning of the mission,  $\beta_0 = \sigma^* A / m_0$ : values of  $\beta_0$ , ranging from 0 (pure SEP) to 0.05 can be assumed for near- to mid-term technology [8].  $m_0$  and  $m$  are the spacecraft mass at the beginning of the mission and at any given time, respectively. Note that, in the hybrid case, the spacecraft mass varies in general, due to the SEP propellant consumption, and so does the acceleration from the sail.  $\sigma^* \cong 1.53 \cdot 10^{-3} \text{ kg/m}^2$  is the critical sail loading for the Sun.

The sail acceleration is controlled through its attitude: the vector  $\hat{\mathbf{n}}$  can be described using the so-called *cone angle*  $\alpha$  (angle between  $\hat{\mathbf{n}}$  and  $\hat{\mathbf{r}}_1$ , see Fig. 1b) and the *clock angle*  $\delta$  (angle measured around  $\hat{\mathbf{r}}_1$ , starting from the vertical plane, of the component of  $\hat{\mathbf{n}}$  perpendicular to  $\hat{\mathbf{r}}_1$ , see Fig. 1c). In the hybrid spacecraft, thin film solar cells (TFSC) cover an area  $A_{TF} = 0.05A$  on the sail, and are used to power the SEP thruster. The area ratio is a conservative estimation based on previous studies [2]. The actual direction of the acceleration  $\hat{\mathbf{m}}$  is related to  $\hat{\mathbf{n}}$  through the coefficients  $g$  and  $h$  [2], that can be computed as a function of the reflectivity of the sail,  $\tilde{r}_s = 0.9$ , and of the thin film  $\tilde{r}_{TF} = 0.4$  [1]:

$$g = 1 + \tilde{r}_s + \frac{A_{TF}}{A} (\tilde{r}_{TF} - \tilde{r}_s); \quad h = 1 - \tilde{r}_s - \frac{A_{TF}}{A} (\tilde{r}_{TF} - \tilde{r}_s) \quad (2)$$

The thrust of the SEP is assumed to be variable and mounted on a gimbal, and thus steerable. This adds three more controls to the spacecraft: thrust direction and magnitude. The propellant mass flow  $\dot{m}$  is related to the thrust through the Newton's law and the conservation of mass:

$$\dot{m} = T / I_{sp} g_0 \quad (3)$$

where we consider a specific impulse  $I_{sp} = 3200 \text{ s}$  (based on current ion engine technology (existing NSTAR/DS1 [9]) and  $g_0 = 9.81 \text{ m/s}^2$ .

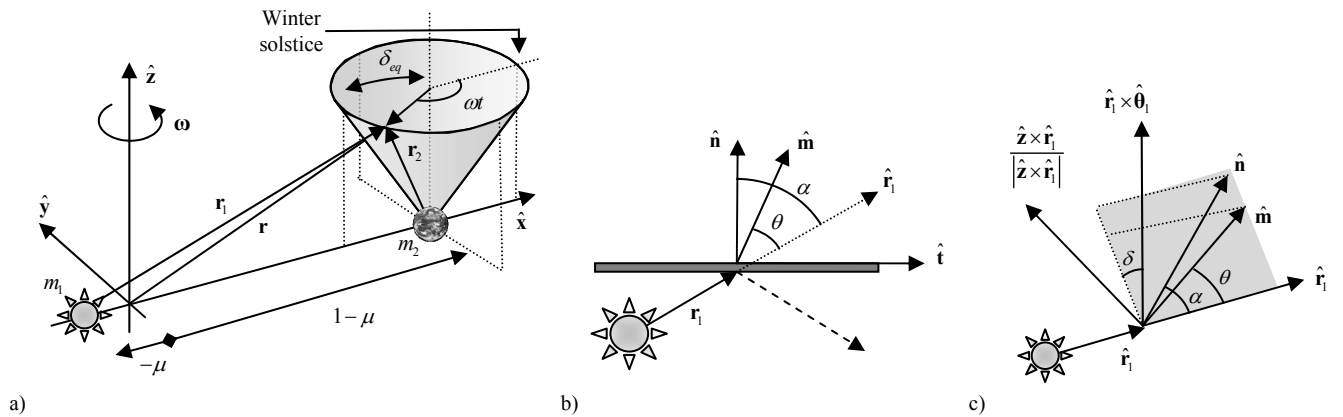


**Fig. 1. a) Restricted three-body problem and pole-sitter reference. b) Definition of the cone and center-line angles (plane of the figure is perpendicular to the sail, containing the Sun vector  $\mathbf{r}_1$ ). c) Solar sail cone and clock angles.**

## 2. POLE-SITTER ORBITS

A pole-sitter spacecraft is constantly aligned with the polar axis of the Earth. We can consider that the polar axis of the Earth does not change its direction while the Earth is orbiting the Sun. In the synodic reference frame, the same axis rotates with a motion of apparent precession: its angular velocity is  $-\boldsymbol{\omega}$  (refer to Fig. 1a). Therefore the polar axis spans a full conical surface every year. The cone half angle is the tilt of the axis relative to the ecliptic, i.e.  $\delta_{eq} = 23.5$  deg. The position of the spacecraft is to be constrained, to follow the apparent precession of the polar axis, and hence maintain the pole-sitter condition. It is assumed that the spacecraft is injected at time  $t_0 = 0$  at the winter solstice, and therefore the pole-sitter is on the cone at position:

$$\mathbf{r}(t) = \begin{bmatrix} d(t) \sin \delta_{eq} \cos \omega t + (1 - \mu) & -d(t) \sin \delta_{eq} \sin \omega t & d(t) \cos \delta_{eq} \end{bmatrix}^T \quad (4)$$

where  $d(t)$  is the distance from the centre of the Earth, and is a continuous function of time. The North Pole case is considered.

In this work, we search for optimal periodic pole-sitter orbits, that minimize the SEP propellant consumption over a period (one year), while maintaining the pole-sitter condition (4) at each time during the mission. Optimal orbits are defined in terms of evolution over one year of the states (position, velocity, mass), and controls (sail cone and clock angles, SEP thrust direction and magnitude). The optimization process is performed in two steps: the first, which aims at finding a first guess solution, and the second, which locally optimizes the first guess. Details of the optimization process are not covered in this paper, being subject of another publication [10]. Here we provide a brief outline of the procedure. The first guess is generated by using a shape-based approach, in which a specific orbit for the spacecraft and initial mass  $m_0$  are assigned, and then the controls that enable that orbit are obtained from the equations of motion, with an iterative process. The orbit is discretized into a finite number of points in time. At each point, the sail cone and clock angles are computed numerically, minimizing the magnitude of the SEP acceleration. Once  $\mathbf{a}_s$  is known,  $\mathbf{a}_T$  can be computed by differencing. Assuming that the thrust remains constant from one point to the next along the orbit, Eq. (3) can be integrated to find the mass change. With this new value of mass, the procedure iterates on the next point on the orbit. The subsequent optimal control problem finds the orbit  $\mathbf{r}(t)$  and the control history that minimizes the propellant consumption of the spacecraft after one orbital period, subject to the boundary condition of periodicity and the pole-sitter constraint (4). A direct method based on pseudo-spectral discretization is used: the tool, named PSOPT, was created and coded in C++ and is freely available to use [11]. Note that the solutions found through the shape-based approach do not, in general, minimize propellant consumption. However, it was verified that, if the shape based approach is used on an orbit that is the result of an optimization, the control history, and thus also the propellant mass, is very similar to the optimal one. Some examples of pole-sitter orbits are plotted in Fig. 2: (a) shows the directions of the acceleration vectors (sail, SEP thrust and total) and sail normal along a constant-distance orbit; (b) shows a family of optimal orbits, found solving the optimal control problem.

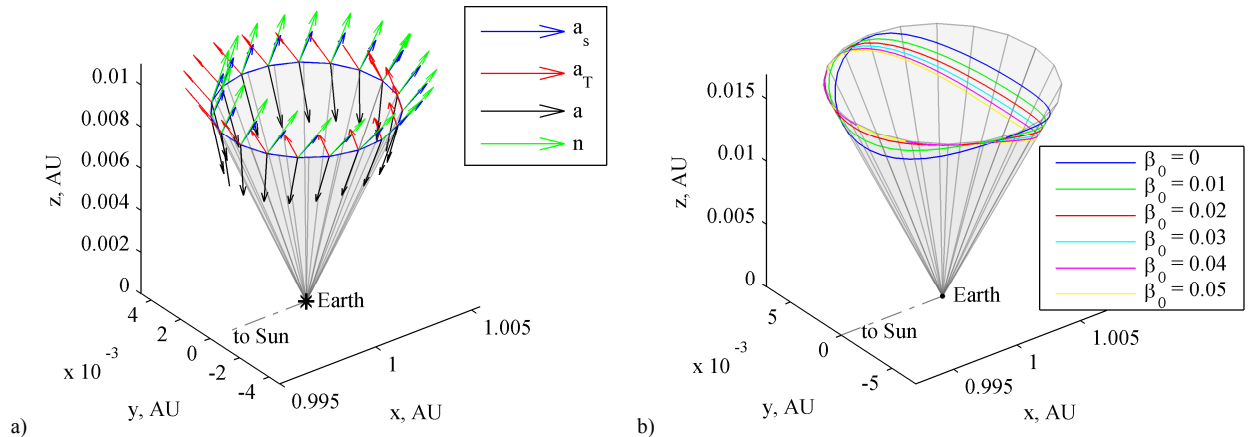


**Fig. 2. a) Acceleration vectors and sail normal along a constant-distance pole-sitter orbit. b) A family of optimal orbits, constrained to less than 0.01831 AU from the Earth, for different values of  $\beta_0$ .**

### 3. MASS BUDGET

By comparing optimal solutions for pure SEP and hybrid spacecraft, it is found that the latter requires a lower propellant mass fraction. However, it is a more complex system, mainly due to the presence of the solar sail and the need to have a gimballed thruster. Due to the additional subsystem mass, we need to assess the conditions at which the hybrid system allows a greater payload mass  $m_{pl}$ , with the same initial spacecraft mass  $m_0$ , or vice-versa a smaller launch mass for the same payload.

For sake of comparison, the technological assumptions are based on those chosen in [2]. In that work, the authors computed the requirements for a spacecraft to be stationary in the Sun-Earth rotation frame, placed at 0.01831 AU above the North Pole at the summer solstice (hence above the Lagrange point  $L_1$ ). Here the distance is constrained to be less than or equal to this value, for consistency, leading to optimal orbits like those in Fig. 2b.

For a preliminary mass budget, the total spacecraft mass can be split as:

$$m_0 = m_{prop} + m_{tank} + n_{thrusters} (m_{SEP} + m_{gimbal}) + m_s + m_{TF} + m_{pl} \quad (5)$$

where  $m_{prop}$  is the propellant mass necessary for a given mission duration  $t_{mission}$ . The mass of the tanks is a function of the propellant mass [12]:  $m_{tank} = 0.1m_{prop}$ . Two thrusters were considered for redundancy,  $n_{thrusters} = 2$ . The mass of the engine is function of its power, though  $m_{SEP} = k_{SEP} P_{SEP,max}$ , with  $k_{SEP} = 20 \text{ kg/kW}$  (NASA solar electric propulsion technology application readiness class engine [9]). The maximum power  $P_{SEP,max}$  required by the SEP subsystem is computed as a function of the maximum thrust  $T_{max}$  required during the mission, as  $P_{SEP,max} = T_{max} v_e / 2\eta_{SEP}$ , where  $\eta_{SEP} = 0.7$  is the efficiency of converting electrical energy [13]. For the hybrid spacecraft,  $m_{gimbal} = 0.3m_{SEP}$  [12]; for the pure SEP, instead,  $m_{gimbal} = 0$ , because the thruster is fixed with the spacecraft bus. The total sail area (highly reflective surface + TFSC) can be computed starting from the assumed values of  $\beta_0$  and  $m_0$ . The mass of the thin film is proportional to its area:  $m_{TF} = \sigma_{TF} A_{TF}$ , where  $\sigma_{TFSC} = 100 \text{ g/m}^2$  [1]. The area of the thin film can be estimated as a function of the maximum power. For the pure SEP spacecraft, the solar panels are usually kept perpendicular to the Sun vector, and therefore the area of TSFC necessary to guarantee the required power is  $A_{TF} = P_{SEP,max} / W\eta_{TF}$ , with  $\eta_{TF} = 0.05$  due to the relatively low efficiency of the thin film, and energy flux density of the Sun  $W = 1367 \text{ W/m}^2$  at 1 AU. In the hybrid spacecraft, instead, the TFSC is part of the reflective surface, and therefore its pitch with respect to the Sun vector is given by the clock angle of the sail  $\alpha = \alpha_{T_{max}}$  at the instant when the maximum thrust is required. Consequently, in the hybrid case, the area of the TFSC shall be augmented according to  $A_{TF} = P_{SEP,max} / W\eta_{TF} \cos \alpha_{T_{max}}$ . The area of the sail is simply  $A_s = A - A_{TF}$ , and its mass is  $m_s = \sigma_s A_s$ .  $\sigma_s$ , the mass per unit area of the sail, or *sail loading*, which is a critical parameter that depends on the solar sail technology. It is expected that near-term technological developments should allow values of  $10 \text{ g/m}^2$  [14]. Ultra-thin (around  $2 \mu\text{m}$  of thickness) sails are expected in the mid- to long-term timeframe [15]: they can lead, for large sails, to loadings of the order of  $5 \text{ g/m}^2$ .

Eq. (5) allows us to implicitly find  $m_0$  for a given payload mass  $m_{pl}$ . Given a guess value for the initial mass  $m_0 = m_{0,guess}$ , firstly the optimal 1-year periodic orbit is determined solving the optimal control problem. This orbit is then used to compute the  $m_{prop}$  for the entire mission duration, using the shape-based method. An iterative Newton-Raphson method is used to solve Eq. (5): at every iteration the propellant mass and the mass of all the other subsystems are re-computed, leading to a new value of  $m_0$ , until convergence.

Fig. 3 shows the initial mass of the spacecraft needed for  $m_{pl} = 100 \text{ kg}$ , as a function of the lightness number  $\beta_0$ , and for two values of  $\sigma_s$ :  $7.5 \text{ g/m}^2$  and  $5 \text{ g/m}^2$ . The pure SEP case is also represented, when feasible, as a dot along  $\beta_0 = 0$ . For comparison with the hybrid cases, dashed horizontal lines were added. Different colors refer to different mission durations, from 5 to 10 years.

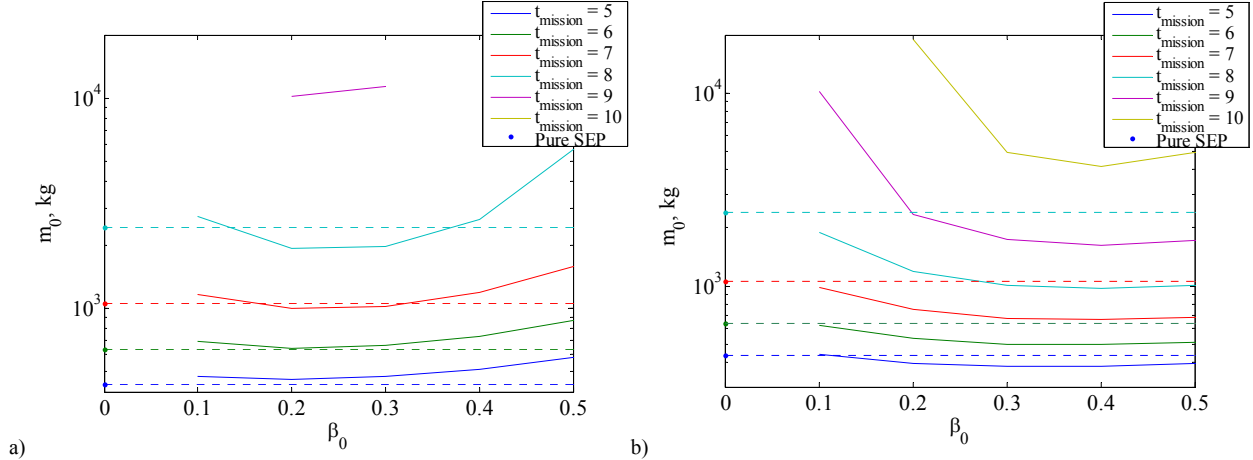


**Fig. 3. Initial mass required for a 100 kg payload, for pure SEP and hybrid spacecraft as a function of  $\beta_0$ . a)  $\sigma_s = 7.5 \text{ g/m}^2$ ; b)  $\sigma_s = 5 \text{ g/m}^2$ . Pure SEP value extended (dashed line) for comparison with hybrid.**

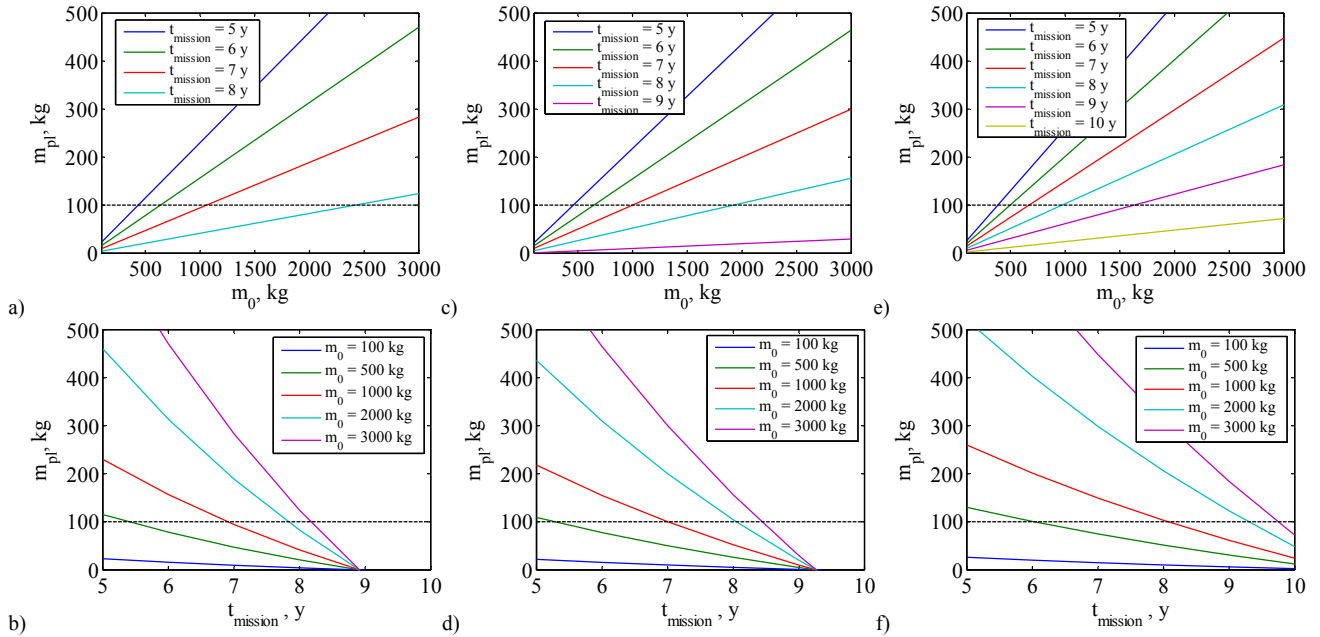


**Fig. 4. Payload mass as a function of initial mass and mission duration. a), b) Pure SEP spacecraft; c), d) Hybrid spacecraft with  $\sigma_s = 7.5 \text{ g/m}^2$  and  $\beta_0 = 0.02$ ; e), f) Hybrid spacecraft with  $\sigma_s = 5 \text{ g/m}^2$  and  $\beta_0 = 0.04$ .**

It is interesting to note that not all the mission durations are achievable with a given  $\beta_0$ : for example, the solution with pure SEP does not exist for missions of 9 years and longer. In the same way, if the sail loading is  $7.5 \text{ g/m}^2$ , then only solutions with  $0.02 < \beta_0 < 0.03$  exist, and no solution exists for longer missions.

The trade-off between payload mass, mission duration and initial mass is presented in Fig. 4, for different types of spacecraft: Fig. 4 (a) and (b) refer to a pure SEP; (c) and (d) to a near-term hybrid sail; finally, (e) and (f) to a far-term hybrid spacecraft. It can be seen that the system mass scales linearly with the payload mass, and that the introduction of the sail enables longer lifetimes.

## CONCLUSIONS

In this paper, we designed optimal pole-sitter orbits (spacecraft constantly above the a pole of the Earth) with a hybrid solar electric propulsion (SEP) and solar sail system. Then, we investigated when a hybrid spacecraft

enables not only fuel saving, but a smaller initial spacecraft mass with respect to the pure SEP case. It was found that, with near- to mid-term sail technology, the hybrid spacecraft has a lower initial mass than the SEP case if the mission duration is 7 years or more, with higher benefit for longer missions. Assuming long-term sail technology, then the hybrid spacecraft outperforms the pure SEP case even for short missions.

Moreover, it was found that the system mass scales linearly with the payload mass; however, the lifetime is limited by the type of propulsion system, no matter the initial mass: the pure SEP is infeasible for missions longer than 8 years, while the addition of a solar sail extends the mission time. It is therefore proposed that a hybrid solar sail and SEP system may be a means of enabling challenging long-duration, high energy missions by using a modest solar sail to enhance the performance of existing SEP technology.

## ACKNOWLEDGMENTS

This work was funded by the European Research Council, as part of project 227571 VISIONSPACE. The authors thank Dr. Victor M. Becerra, of the School of Systems Engineering, University of Reading, Reading, UK for providing the software PSOPT freely, as well as advices on its use.

## REFERENCES

1. M. Leipold, M. Götz, “Hybrid photonic/electric propulsion”, Kayser-Threde GmbH, Munich, Germany, 2002.
2. S. Baig, C. R. McInnes, “Artificial three-body equilibria for hybrid low-thrust propulsion”, *Journal of Guidance, Control, and Dynamics*, vol. 31, n. 6, p. 1644-1655, 2008. DOI: 10.2514/1.36125
3. G. Mengali, A. A. Quarta, “Trajectory design with hybrid low-thrust propulsion system”, *Journal of Guidance, Control, and Dynamics*, vol. 30, n. 2, p. 419-426, 2007. DOI: 10.2514/1.22433
4. J. Simo, C. R. McInnes, “Displaced periodic orbits with low-thrust propulsion”, in *Proceedings of 19<sup>th</sup> AAS/AIAA Space Flight Mechanics Meeting*, Georgia, USA, 2009.
5. O. Mori, H. Sawada, R. Funase, T. Endo, M. Morimoto, et al., “Development of first solar power sail demonstrator - IKAROS”, in *Proceedings of 21st International Symposium on Space Flight Dynamics, ISSFD 2009*, Toulouse, France, 2009.
6. J. M. Driver, “Analysis of an arctic polesitter”, *Journal of Spacecraft and Rockets*, vol. 17, n. 3, 1980. DOI: 10.2514/3.57736
7. C. R. McInnes, “Solar sailing: technology, dynamics and mission applications”, *Springer-Praxis books in astronautical engineering*, ed. J. Mason, Springer-Verlag, Berlin, 1999. ISBN: 3-540-21062-8
8. B. Dachwald, G. Mengali, A. A. Quarta, M. Macdonald, “Parametric model and optimal control of solar sails with optical degradation”, *Journal of Guidance, Control, and Dynamics*, vol. 29, n. 5, p. 1170-1178, 2006. DOI: 10.2514/1.20313
9. J. Brophy, “Advanced ion propulsion systems for affordable deep-space missions”, *Acta Astronautica*, vol. 52, p. 309-316, 2003. DOI: 10.1016/S0094-5765(02)00170-4
10. M. Ceriotti, C. R. McInnes, “An Earth pole-sitter using hybrid propulsion”, in *Proceedings of AIAA/AAS Astrodynamics Specialist Conference*, Toronto, Ontario, Canada, 2010.
11. V. M. Becerra, “PSOPT optimal control solver user manual”, <http://code.google.com/p/psopt>, 2009.
12. R. Gershman, C. Seybold, “Propulsion trades for space science missions”, *Acta Astronautica*, vol. 45, n. 4-9, p. 541-548, 1999. DOI: 10.1016/S0094-5765(99)00174-5
13. S. Kitamura, Y. Ohkawa, Y. Hayakawa, H. Yoshida, K. Miyazaki, “Overview and research status of the JAXA 150-mN ion engine”, *Acta Astronautica*, vol. 61, n. 1-6, p. 360-366, 2007. DOI: 10.1016/j.actaastro.2007.01.010
14. B. Dachwald, “Solar sail performance requirements for missions to the outer solar system and beyond”, in *Proceedings of 55<sup>th</sup> International Astronautical Congress (IAC 2004)*, Vancouver, Canada, 2004.
15. D. M. Murphy, T. W. Murphey, P. A. Gierow, “Scalable solar-sail subsystem design considerations”, in *Proceedings of 43<sup>rd</sup> Structures, Structural Dynamics, and Materials Conference*, Denver, Colorado, 2002.